



Superconducting Magnet Division

Magnet Note

Author: B. Parker
Date: June 14, 2004
Topic No: 637-40 (AM-MD-337)
Topic: Linear Collider Final Focus
Title: Compensation of the Effects of Detector Solenoid on the Vertical Beam Orbit in NLC

M. Anerella	S. Ozaki
J. Cozzolino	B. Parker
J. Escallier	S. Peggs
G. Ganetis	F. Pilat
M. Garber	S. Plate
A. Ghosh	C. Porretto
R. Gupta	W. Sampson
H. Hahn	J. Schmalzle
M. Harrison	J. Sondericker
J. Herrera	S. Tepikian
A. Jain	R. Thomas
P. Joshi	D. Trbojevic
S. Kahn	P. Wanderer
W. Louie	J. Wei
J. Muratore	E. Willen



Compensation of the Effects of Detector Solenoid on the Vertical Beam Orbit in NLC

Brett Parker

Brookhaven National Laboratory
P.O.Box 5000, Upton, NY 11973

Andrei Seryi

Stanford Linear Accelerator Center
P.O.Box 20450, Stanford, CA 94309

Abstract: In this note we consider compensation of the vertical angle at the IP that arises when the NLC beam enters the detector solenoid. While this angle is antisymmetric for e^+e^- collisions and does not affect luminosity, compensating this angle is desirable to guarantee knowledge of polarization at the IP. For the e^-e^- case compensation is necessary also from the luminosity point of view. We show in this note that the most effective compensation can be done locally, with a special dipole coil arrangement incorporated into the detector. It is shown that compensation can be achieved for both e^+e^- and e^-e^- case and that this scheme is compatible with beam size compensation by both the standard method, using skew quadrupoles, and by means of more advantageous method using weak antisolenoids.

Compensation of the Effects of Detector Solenoid on the Vertical Beam Orbit in NLC

BRETT PARKER¹ AND ANDREI SERGI²

¹ Brookhaven National Laboratory, P.O.Box 5000, Upton, NY 11973

² Stanford Linear Accelerator Center, P.O.Box 20450, Stanford, CA 94309

LCC-NOTE-0143 AND SLAC-TN-04-044
BNL-MDN-637-40 AND BNL-AM-MD-337

June 3, 2004

Abstract

In this note we consider compensation of the vertical angle at the IP that arises when the NLC beam enters the detector solenoid. While this angle is antisymmetric for e^+e^- collisions and does not affect luminosity, compensating this angle is desirable to guarantee knowledge of polarization at the IP. For the e^-e^- case compensation is necessary also from the luminosity point of view. We show in this note that the most effective compensation can be done locally, with a special dipole coil arrangement incorporated into the detector. It is shown that compensation can be achieved for both e^+e^- and e^-e^- case and that this scheme is compatible with beam size compensation by both the standard method, using skew quadrupoles, and by means of more advantageous method using weak antisolenoids.

1 Introduction

The beam entering the Interaction Region (IR) with horizontal crossing angle will deviate in the vertical plane. Let's first consider a detector solenoid with sharp edges. The vertical orbit is driven by the edge kick $\Theta = \theta_c B_0 L / (2B\rho)$, which occurs when the beam enters the solenoid at radial offset $\theta_c L$, and by the linearly distributed body kick. Here θ_c is half of the crossing angle, L is half length of the detector solenoid, B_0 – solenoid field, $B\rho = pc/e$. The body kick integrated from the solenoid entrance to the Interaction Point (IP) is equal -2Θ , which is twice the edge kick. Since the body kick has twice shorter lever arm, the resulting vertical offset at the IP cancels exactly (see also [1] for a rigorous proof), but the remaining vertical angle at the IP is nonzero and equals $-\Theta$. Correspondingly, the vertical angle of the extracted beam is -2Θ .

In case of e^+e^- collisions the vertical angle of the opposite beam will be antisymmetric, and the beams will collide head on. So, from the luminosity point of view, this angle is of no concern. In the e^-e^- case the trajectories are symmetric and the vertical crossing would need to be compensated to preserve the luminosity. However, in either the e^+e^- or e^-e^- cases, compensation of the vertical angle at the IP is desirable from the point of view of preservation of the knowledge on the beam polarization.

Below we will consider such compensation, and will show that local compensation with a dipole coil integrated with the detector solenoid presents an optimal solution. We will also consider the vertical angle of the extracted beam, that needs to be compensated as well, to allow for post-IP polarization diagnostics and also to align the beam into the extraction line independent of beam energy.

Finally, we will show that such IP vertical angle compensation is compatible with beamsizes compensation by means of antisolenoids [2], which represent a superior strategy in comparison with the standard (by means of skew quads) technique of beamsizes compensation.

2 IP Angle Compensation in a Solenoid with Sharp Edges

Let's consider a specific example. Assume that half solenoid length is $L = 3$ m, half crossing angle is $\theta_c = 10$ mrad, maximum field $B_0 = 5$ T, beam energy 250 GeV. In this case the characteristic angle Θ is approximately $45 \mu\text{rad}$. Corresponding beam trajectories are shown in Fig. 1. One can see that IP offset is zero but the IP angle is not, and symmetry is different for e^+e^- and e^-e^- cases. If we want to introduce some compensating field which would zero the vertical IP angle without changing the IP offset, we need at least two kicks per side.

It is interesting to note that direction of the transverse field seen by a particle and the direction of the required compensation field do not depend on the particle charge. Therefore compensation will work both for e^+e^- and e^-e^- cases. The symmetry of trajectories will be however defined by the charges of particles.

Let's assume that compensating kicks are located at $L_1 = 2$ m and $L_2 = 5$ m. The kicks needed to compensate the IP are given by $K_1 = \Theta/(1 - L_1/L_2)$ and $K_2 = -\Theta/(L_2/L_1 - 1)$ which are $75 \mu\text{rad}$ and $-30 \mu\text{rad}$ in our case. The compensated trajectories corresponding to our example are shown in Fig. 2.

Note that the inner kicks act on both the incoming and outgoing beams, but the outer kicks act on incoming beam only. Therefore, the vertical angle of the extracted beam is increased by the value of one outer kick and thus given by $-\Theta(2 + 1/(L_2/L_1 - 1))$ which is $-120 \mu\text{rad}$ instead of $-90 \mu\text{rad}$ in the case without IP angle compensation. Inside the detector, the transverse field acting on the outgoing disrupted beam is increased by the value of the inner kick.

To facilitate extraction of the beam, and also to make possible the downstream polarization diagnostics, the vertical angle of the outgoing beam can be corrected by a vertical bend (or offset of the first quadrupole of the extraction line). Fig. 3 shows the extracted beam trajectory without IP angle compensation, and Fig. 4 corresponds to the case when both the IP angle, and extracted beam angle are corrected.

3 IP Angle Compensation in the NLC Silicon Detector

The ANSYS model of Silicon Detector (SiD), the fields and locations of the Final Doublet (FD) focusing elements of the NLC Beam Delivery System are shown in Fig. 5.

In absence of any focusing elements, or if the extent of the detector field is shorter than the distance between Final Doublets, the the vertical trajectory in the detector solenoid would be primarily determined by the horizontal field ($B_r - \theta \cdot B_z$). Corresponding vertical trajectory, obtained by simple integration of the SiD horizontal field, are shown in Fig. 6. Similar as in the case of a sharp edge solenoid, the IP offset is exactly canceled while the IP angle is nonzero. We stress again that the cancellation of the IP offset is an important feature, since it also results in cancellation of the coupling and other beam distortions introduced by the solenoid.

Presence of the focusing elements, and overlap of the solenoid field with final quadrupoles, destroys this perfect cancellation of the orbit and beam distortions. In the case of SiD, the beam orbit obtained by tracking with DIMAD [3] is shown in Fig. 7. One can see that the vertical angle at IP is about $100 \mu\text{rad}$, and that the vertical IP position is not zero (equals to approximately $-20 \mu\text{m}$), due to the aforementioned overlap of solenoid field with final quadrupole QD0 (see [2] for more discussion of the solenoid effects on the beam size).

The vertical trajectory is most curved inside of the detector, 2-3 m from the IP. Thus, an effective compensation must be local. If we were to compensate this IP angle by offsets of the FD quads, as shown in Fig. 8 and Fig. 9, or other bends in FD, the resulting orbit deviation would

be too large and such a solution would not be appropriate, in particular from the point of view of synchrotron radiation.

Local compensation of the IP angles can be done by a pair of dipoles embedded into the detector coil at large radius (couple of meters). Their fields should be antisymmetrical left and right from the IP. Such a field can be created by a novel pair of dipole windings integrated with the detector solenoid (see Fig. 10) in its cryostat, denoted as Detector Integrated Dipole (DID) Corrector (also known as Serpentine corrector corresponding to a particular winding technique, which inspired the idea of local compensation of the IP angles). Design considerations for the DID corrector are given in the next section.

The DID corrector field, optimized to correct the orbits in SiD is shown in Fig. 11. The shape of the field was obtained by calculation with Opera3D code. Note that this field represent one of possible solution for local correction, and the particular field shape is not important as long as it is local to the detector. For this field to compensate the IP angle, it has to be combined with external kicks of different sign, so that the combined field would produce only an angle at the IP, and no offset. We use offsets of FD quadrupoles to produce these external kicks.

Fig. 12 illustrates compensation of the IP angles in SiD using DID Corrector together with offsets of FD quadrupoles QD0 and QF1. (In principle, offset of only the QD0 would be sufficient if we were to worry only about the angle and offset at the IP. As we discuss further below, the QF1 offset is necessary to cancel the vertical second order dispersion). One can see that the combined integrated effect of the DID and quads resembles the effect of the solenoid itself. Trajectories near IP in SiD obtained with tracking are shown in Fig. 13. The IP angle is compensated to less than a μrad . One can see that the orbit deviation near IP is not larger than without any compensation, due to local character of the correction.

The IP beam phase-space of the tracked beam is shown in Fig. 14. In this case the IP orbit is already compensated, but the beam size is still large, mostly due to (yx') coupling and other correlations occurring due to passing through the solenoid field. Note that this increase of the beam size is not attributable to a crossing angle and vertical orbit deviation, since the major term ((yx') coupling) does not depend on the crossing angle but is mostly driven by the fraction of the solenoid field overlapping with the Final Doublet (see more in [2]).

To compensate the beam size distortion due to solenoid crossing, we applied linear knobs to correct the (yx') , (yE) , (yx) and other linear terms using skew quadrupole in FD and the sextupole displacement knobs. The corrected beam is shown in Fig. 15. The beam size is compensated within 3% of the nominal using only the linear tuning knobs. Further correction of the beam size can be achieved with higher order tuning knobs.

As mentioned above, correction of the IP angle results in increase of the transverse field seen by the outgoing disrupted beam going past the IP and increase of the resulting angle of the extracted beam. Fig. 16 shows that the extracted beam vertical angle is about 50% higher than without IP angle correction. The extracted beam angle can be compensated by a single vertical bend. Beam orbit tracked to the IP and past the IP is shown in Fig. 17.

Finally, compensation of the IP angle and position with the DID field together with offsets of the the QD0 and QF1 quadrupoles may generate the first and second order vertical dispersions at the IP. In order to minimize their effect on the beam size, we adjusted the ratio of the QD0 and QF1 offsets in such a way that the second order dispersion is zeroed, and only linear dispersion is generated, see Fig. 18. This latter is taken out by the standard sextupole displacement knobs.

3.1 Detector Integrated Corrector, Design Considerations

We have investigated integrating the dipole correction coils with the cold mass inside the detector solenoid cryostat for three reasons. First and foremost is that a small diameter magnet placed close to the IP would introduce extra radiation lengths of dead material and reduce the detector acceptance. The large diameter dipole corrector coils proposed are quite thin and present only a negligible addition to the already considerable thickness of the solenoid itself.

Secondly interaction of the solenoidal field with the coil ends yields net torques in the horizontal plane that have to be supported in addition to supporting the dipole's own weight. Co-winding the corrector coils with the solenoid in the same cold mass ensures that no new torque has to be passed to the outside world and the corrector weight is again a small perturbation to the solenoid coil supports.

Finally the large dipole coil radius ensures that even for a relatively crude coil configuration the field seen by the colliding beams is very uniform. At the coil longitudinal midpoints and half the coil radius, 1.4 m, field non-uniformity is less than a few parts in ten-thousand and at the beam pipe approaches a few parts-per-million for the coil configurations investigated so far; however, since each dipole coil has a pattern length almost equal to its radius and since there is strong cancellation of the field at the IP symmetry point, the dipole field profile exhibits a marked longitudinal dependence that is nearly independent of the other details of the coil structure.

Our assumed DID corrector coil pattern is shown at the top of Fig. 10. The number of dipole turns is chosen to leave about a meter of straight section as shown. Adding additional turns to the winding pattern quickly becomes counterproductive as then the dipole ends become too long and the increase of transfer function is balanced by the reduction of the straight section length.

Initially we calculated 3d field profiles based upon the positions of each conductor segment in space (i.e. in effect an air coil). In order to evaluate the effect of the solenoid yoke on the field distribution we generated a simplified 3d conductor model by averaging the conductor locations to a smaller number of coil packs and inserted this coil inside a simplified 3d model of the SiD yoke as shown at the bottom of Fig. 10.

Initially we worried that the yoke endcap, that goes down to small radius, might rob too much flux from the body of the DID corrector thereby reducing its efficiency for making a dipole field. But this was not found to happen and in fact the increase of efficiency that comes from the yoke for the body of the magnet more than makes up for loss near the endcap. There is a small discrepancy between our assumed field shape that occurs near the inner edge of the endcap, but overall the results from the 3d field calculations match our heuristically motivated field shape used for tracking very well.

3.2 Compatibility of IP Angle Compensation and Beamsizes Compensation with Antisolenoids

In the above example we considered the standard (with use of skew quads) technique of beamsizes compensation in solenoid. However, this method does not give perfect beamsizes compensation and it is especially difficult to use the standard method at low beam energies. On the other hand, beamsizes compensation with antisolenoids is a superior strategy which provides almost perfect compensation independent of the beam energy [2]. We will show below that the antisolenoid approach is compatible with the DID Corrector method.

As discussed in [2], most of the aberrations due to solenoid are generated because the solenoid field overlaps with final quadrupole and breaks the natural cancelation of coupling and other beam distortions. A short weak solenoid, coaxial with the detector and overlapping with QD0, can be matched to cancel the integral effect of the overlap, and restore cancelation of distortions. Naturally,

this cancelation then works for any beam energy. Fig.19 shows the SiD field and the modified field, with the antisolenoid field added. Such field generates almost no beam distortion.

Naturally, if we want the antisolenoid solution to remain distortion-free when combined with the DID Corrector, the latter should also be made distortion-free. For this purpose, we add one more dipole corrector in the middle of FD and match three parameters (offsets of QD0, QF1 and middle dipole field) to simultaneously cancel the first and second order dispersions and the IP offset produced by the DID Corrector. Fig. 20 shown the acting horizontal fields and the orbit calculated by integration of B_x , and Fig. 21 shows the orbit obtained by tracking. We see that the IP orbit compensation is as good as in the previous case.

The spectacular effect of the antisolenoid on the beam size is shown in Fig. 22 where the IP orbit compensation is already applied, but all linear knobs are zero. The beam size increase is just 30% which is to be compared with the factor of 65 times (Fig. 14) of beam size increase when the antisolenoid was not used. After the linear knobs were applied to correct remaining small correlations, the beam size was corrected to 1% of the nominal beam size which is almost perfect considering that only linear knobs were used, see Fig. 23.

Comparison of the strength of the skew quad in FD and sextupole displacements needed to achieve correction of the linear beam size without and with the antisolenoid is shown in Fig. 24. We see that the required knob strength is much smaller in the case of antisolenoid.

4 Conclusion

A vertical bend can be added near IP to cancel the vertical IP angle created by crossing the solenoid field, and thus compensate the spin motion. To be effective, this bend needs to be incorporated into detector solenoid winding. We presented a solution which uses the DID Corrector, that provides local compensation of the orbit and works both for e^+e^- and e^-e^- cases. We have shown that this method is also compatible with beamsizes compensation with antisolenoids.

5 Acknowledgement

The authors thank John Hodgson for providing ANSYS models of the NLC detectors, Peter Tenenbaum for creation of the DIMAD models of BDS with solenoid, and Yuri Nosochkov and Tor Raubenheimer for very useful discussions.

References

- [1] P. Tenenbaum, J. Irwin, T.O. Raubenheimer, “Beam Dynamics of the Interaction Region Solenoid in a Linear Collider due to a Crossing Angle”, Phys.Rev. Spec. Topics – Acc. and Beams, v. 6, 061001 (2003).
- [2] Yuri Nosochkov and Andrei Seryi, “Compensation of the Effects of NLC Detector Solenoid on the Beam Size at the IP”, LCC-142, June 2004.
- [3] Roger Servranckx, Karl Brown, Lindsay Schachinger, David Douglas, Peter Tenenbaum, “Users Guide To The Program DIMAD”, SLAC-285, Jan 1990, and also the latest version users guide: <http://www.slac.stanford.edu/accel/nlc/local/AccelPhysics/codes/dimad/dimad.pdf> January 4, 2004.

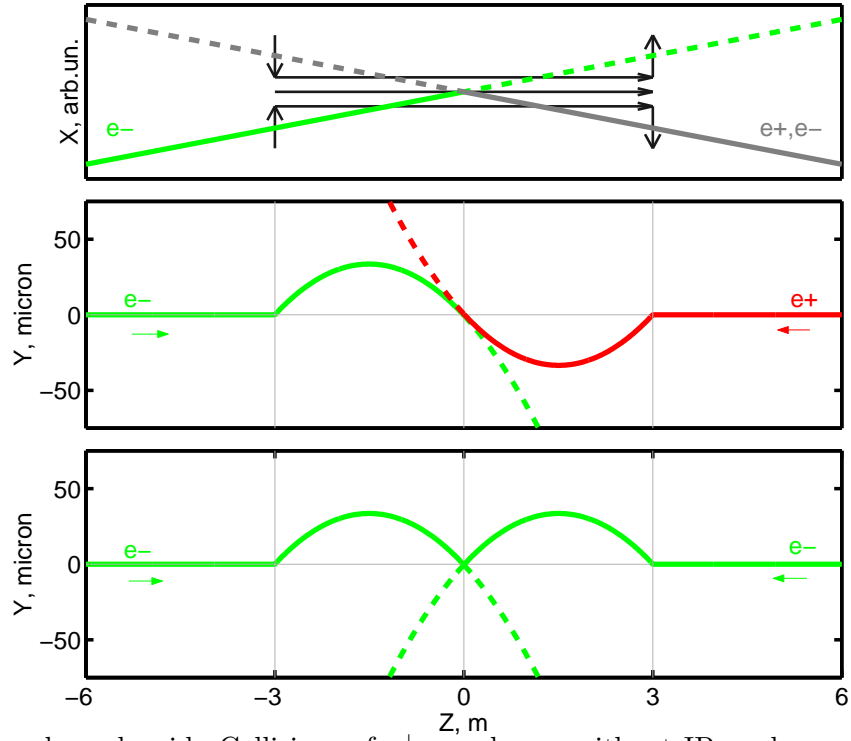


Figure 1: Sharp edge solenoid. Collisions of e^+e^- and e^-e^- without IP angle compensation. $L = 3 \text{ m}$, $\theta = 10 \text{ mrad}$, $B_0 = 5 \text{ T}$, beam energy 250 GeV . Vertical angle at the IP is $45 \mu\text{rad}$.

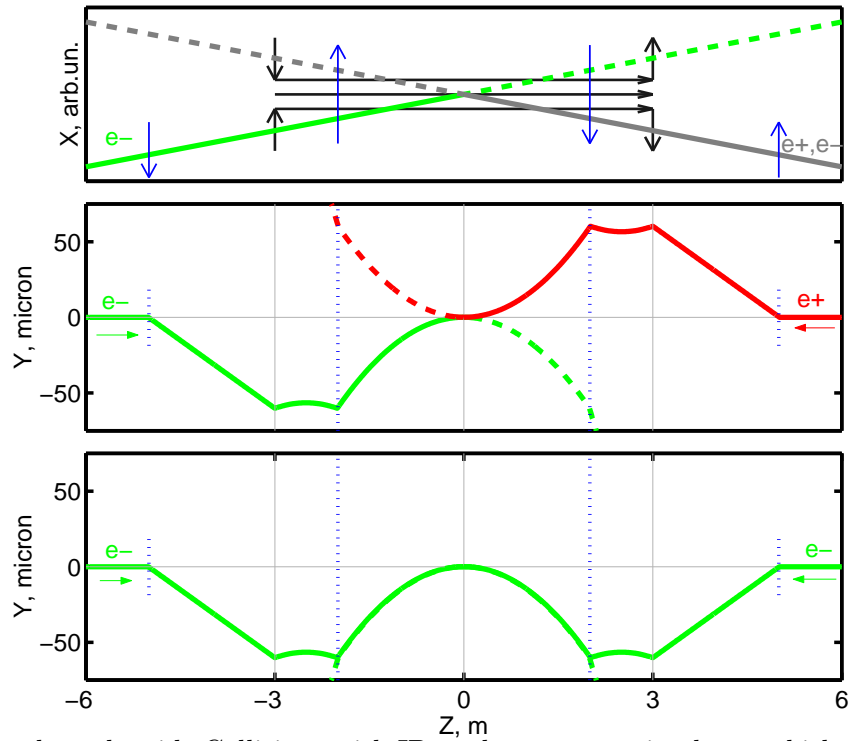


Figure 2: Sharp edge solenoid. Collisions with IP angle compensation by two kicks per side (shown by blue arrows) located at $L_1 = 2 \text{ m}$ and $L_2 = 5 \text{ m}$ with the kick magnitudes $75 \mu\text{rad}$ and $30 \mu\text{rad}$.

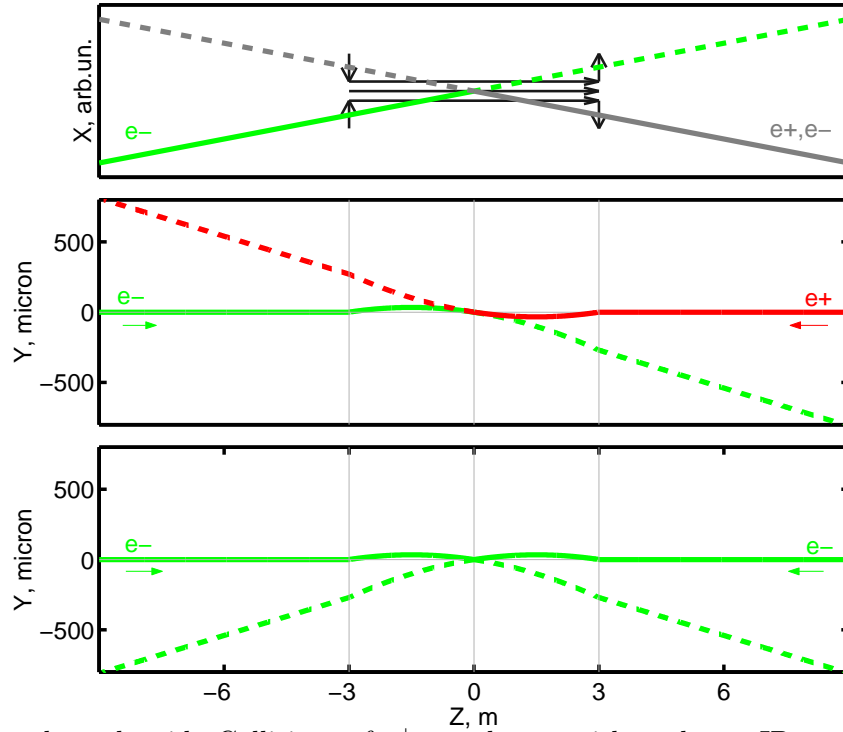


Figure 3: Sharp edge solenoid. Collisions of e^+e^- and e^-e^- without beam IP angle and extracted angle compensation. The angle of the extracted beam is $-90 \mu\text{rad}$

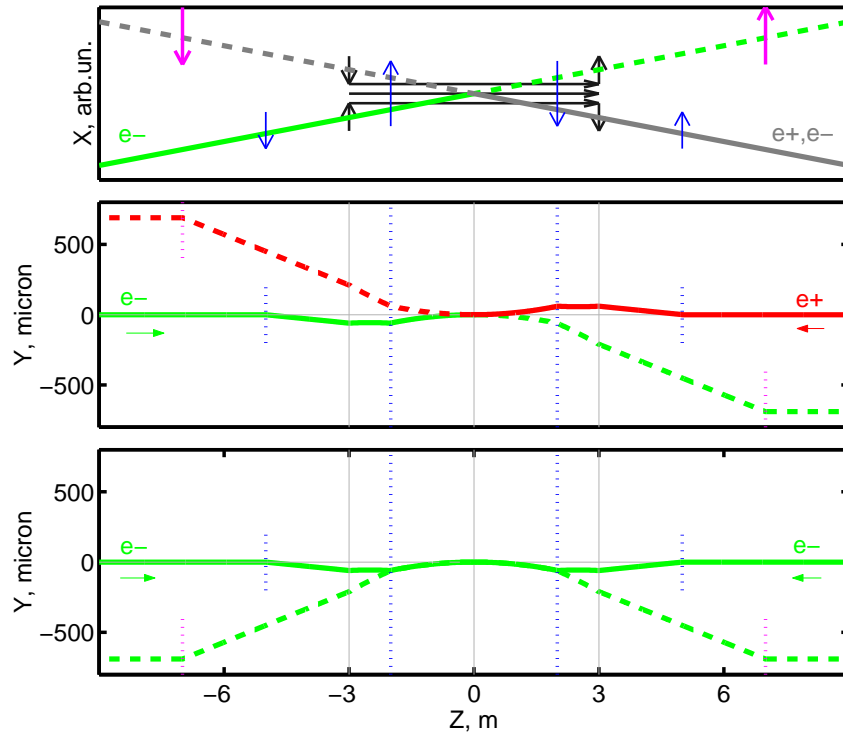


Figure 4: Sharp edge solenoid. Collisions with IP angle compensation and with extraction line angle compensation by a single kick (indicated by magenta arrow) located at $L_3 = 7m$ with kick value of $120 \mu\text{rad}$.

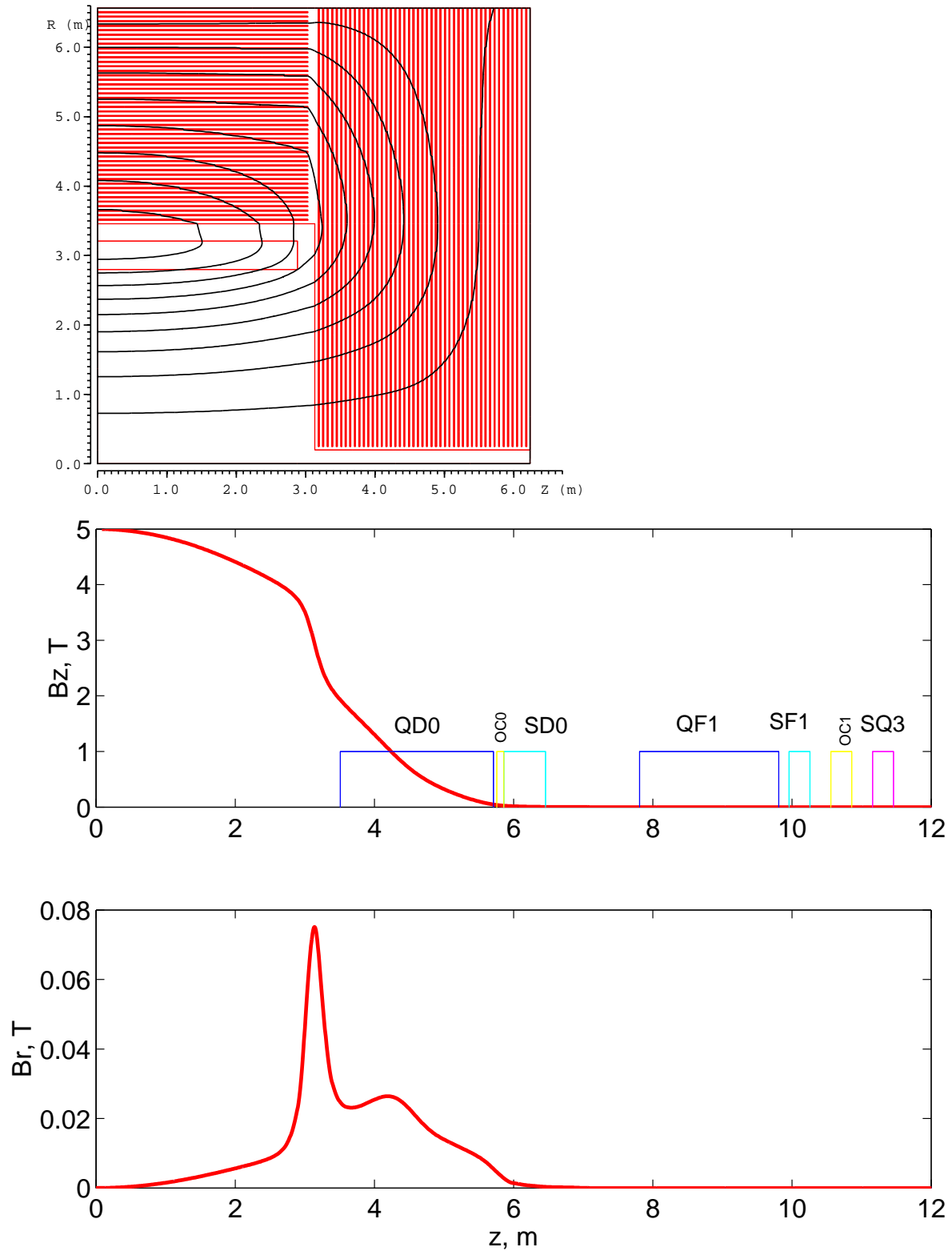


Figure 5: Fields of the Silicon Detector (SiD) calculated by ANSYS (top plot). Longitudinal and radial fields on the ideal beam trajectory with half crossing angle 10 mrad (bottom plots). Locations of the Final Doublet elements are also shown.

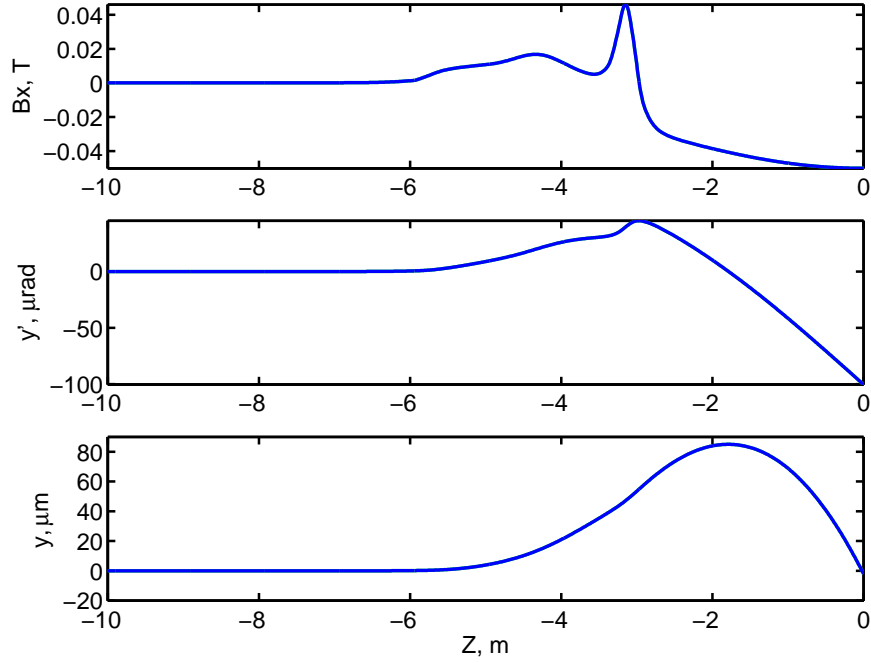


Figure 6: Beam orbit in SiD calculated in assumption of absence of any focusing elements (by simple integration of solenoid B_x). No compensation of the IP angle is applied yet.

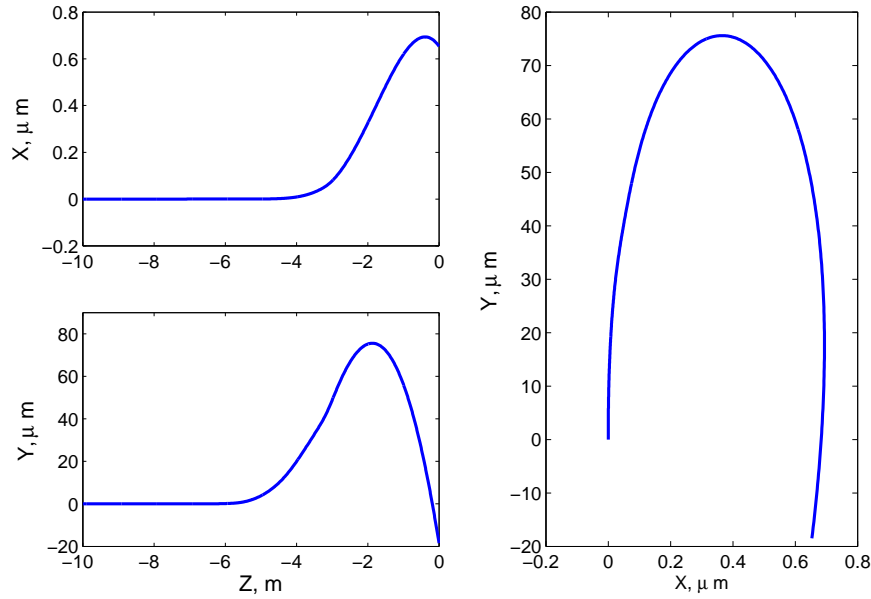


Figure 7: Beam orbit in SiD determined by tracking with DIMAD. No compensation of IP angle applied yet. The IP beam coordinates are: $x = 0.65 \mu\text{m}$, $y = -18.5 \mu\text{m}$, $x' = -0.21 \mu\text{rad}$, $y' = -104 \mu\text{rad}$.

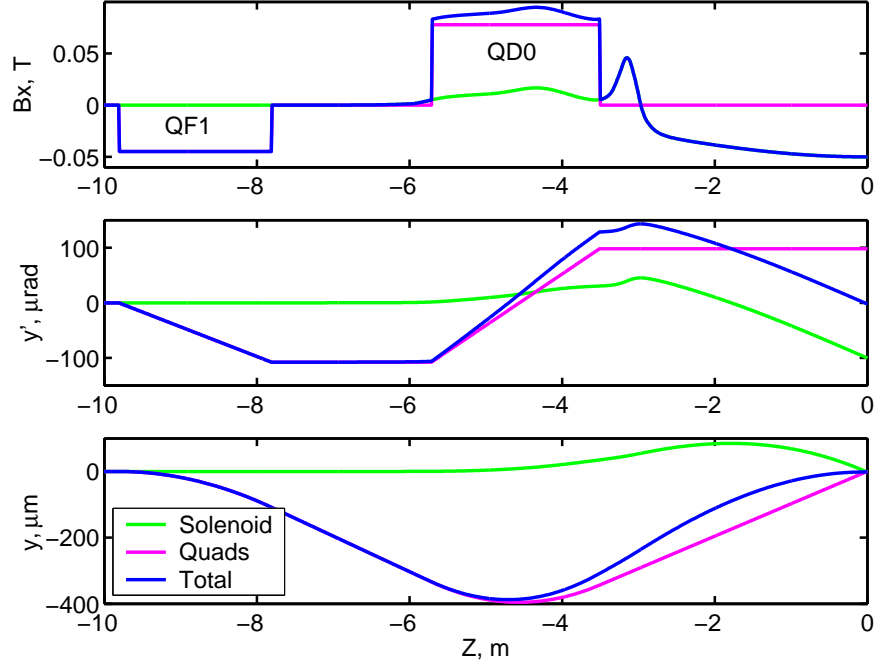


Figure 8: Illustration of the disadvantage of IP angle compensation only by offsets of QD0 and QF1 quadrupoles of the Final Doublet. Horizontal field acting on the beam – top plot, vertical angle – middle plot, position – bottom plot. Contributions of solenoid (which includes both B_r and $B_z \cdot \theta$) and quadrupoles are shown separately. Due to non-local nature of the compensation the resulting deviation of vertical orbit reaches 0.4 mm. (Calculated by integration of B_x , without tracking.)

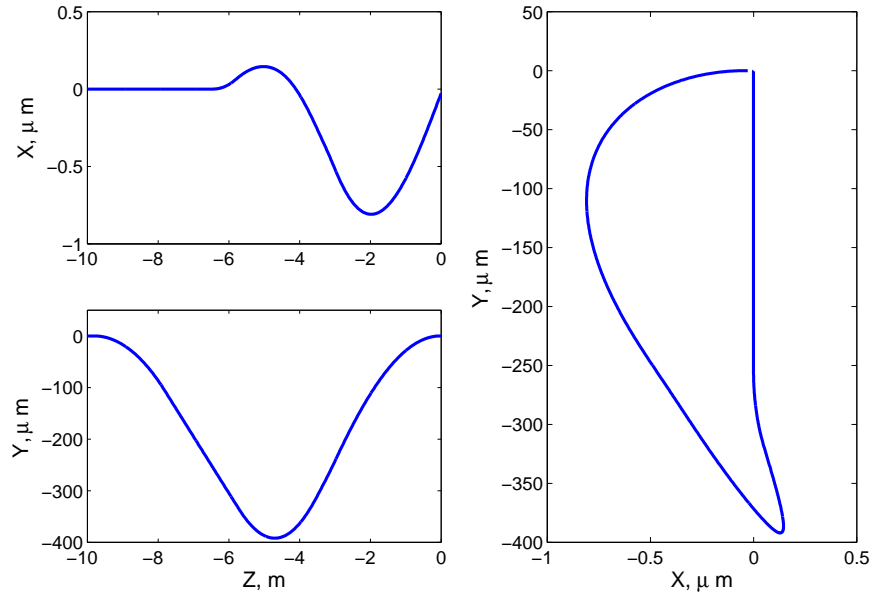


Figure 9: Illustration of the disadvantage of IP angle compensation only by offsets of QD0 and QF1 quadrupoles of the FD. The orbit is calculated by tracking.

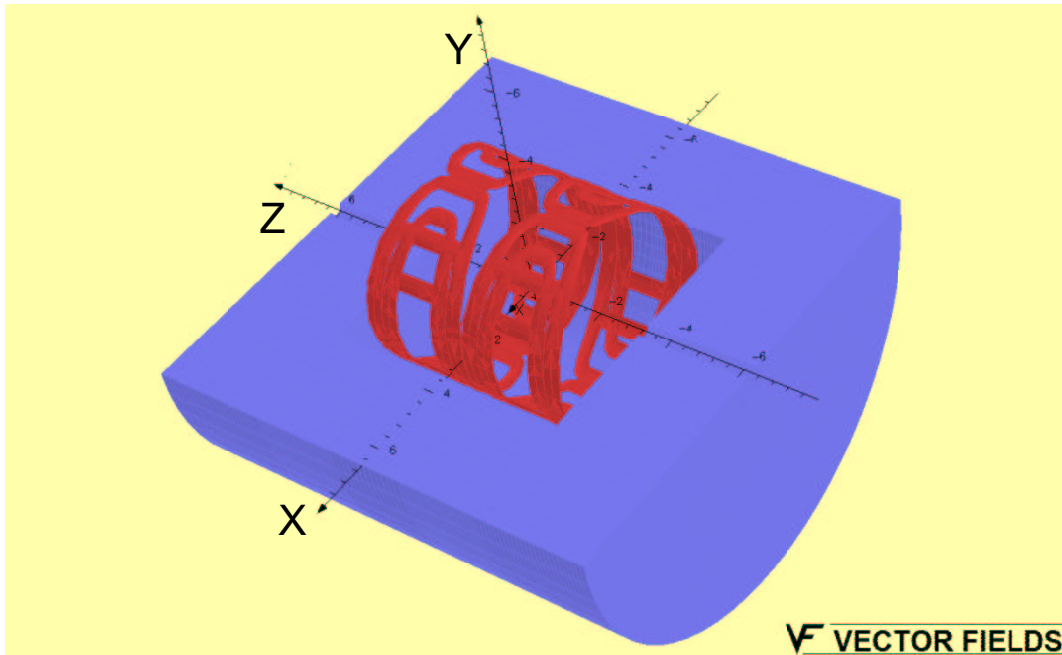
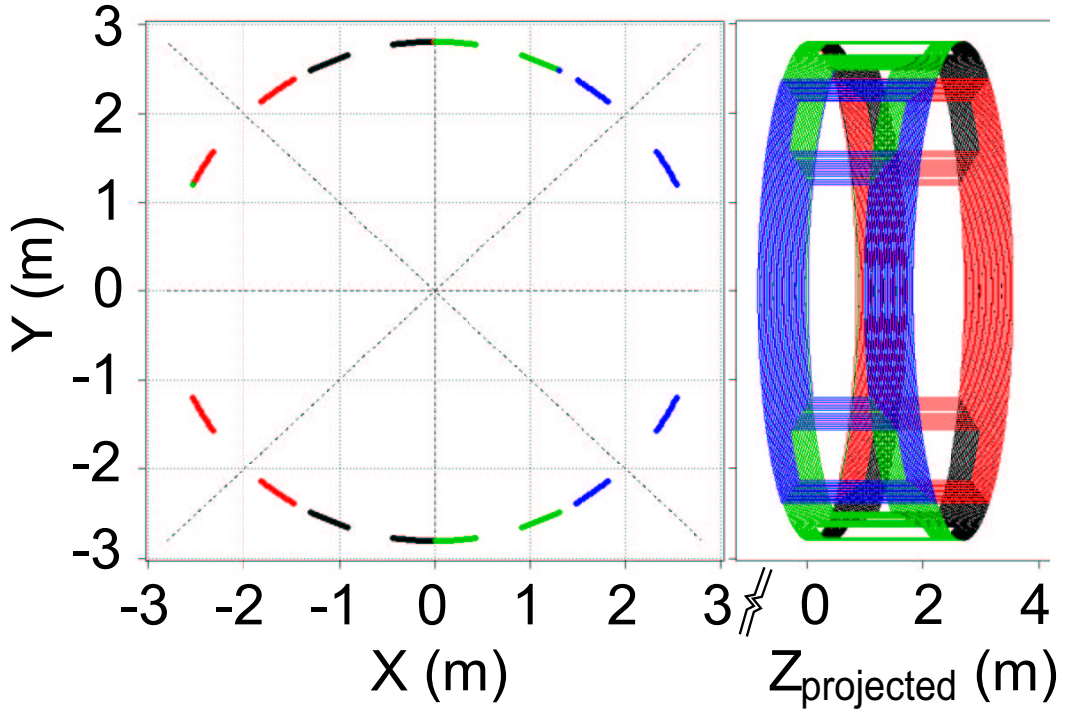


Figure 10: Detector Integrated Dipole (DID) Corrector. The top plot shows the actual arrangement of windings in one half of the corrector and the bottom plot shows a simplified model used for 3D field calculations with Tosca (Opera3D code) to evaluate the effect of iron in the SiD yoke on the dipole field. For ease in viewing the 3D model the solenoid coil and the top half of the SiD yoke are not shown. Except for a small deviation near the start of the endcap around $Z = \pm 3.2$ m the horizontal B_x field profile is very close to that assumed for tracking shown in Fig. 11.

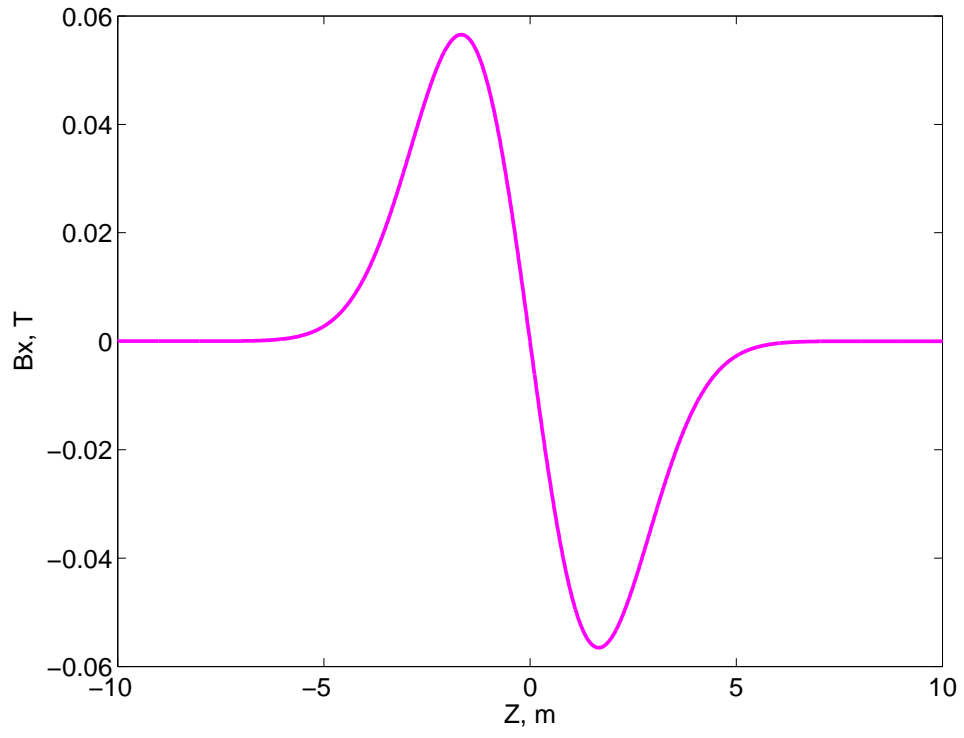


Figure 11: Horizontal field of the DID Corrector optimized to correct the orbits in SiD.

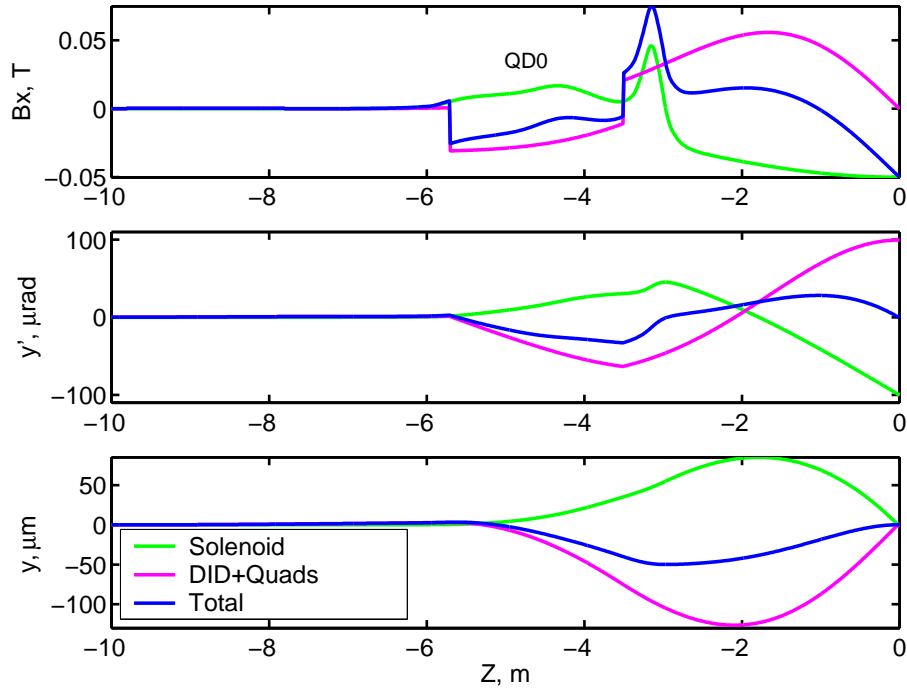


Figure 12: Beam orbits in SiD determined by integration of B_x , without tracking. The IP angle is compensated by the DID Corrector and offsets of QD0 and QF1 quadrupoles.

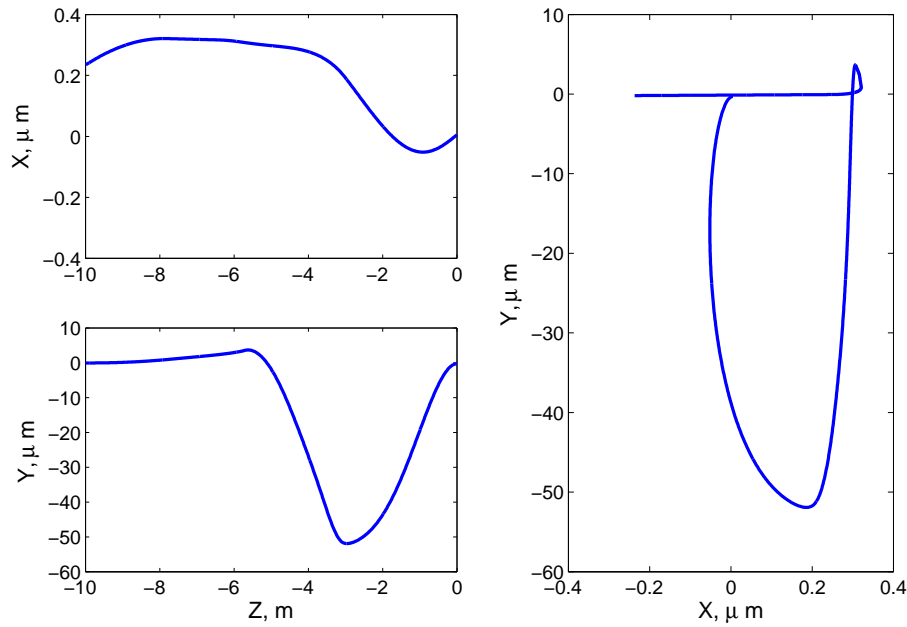


Figure 13: Beam orbits in SiD determined by tracking. The IP angle is compensated by the DID Corrector and offsets of QD0 and QF1 quadrupoles.

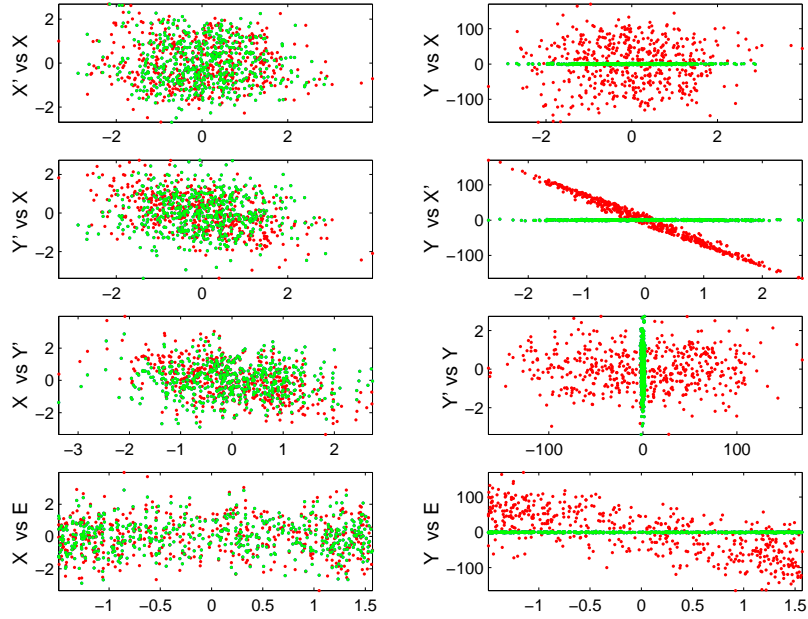


Figure 14: Beam phase-space at the IP determined by tracking (500 rays), normalized to nominal beam size. Green dots show the ideal beam with solenoid field zeroed, and red dots show the beam corresponded to the case when the IP angle is compensated by the DID and offsets of QD0 and QF1 quadrupoles, but the beam size is not yet corrected. The beam sizes are $\sigma_x/\sigma_{x0} = 1.15$, $\sigma_y/\sigma_{y0} = 65$, and major linear correlations are: $\langle yx' \rangle = -58$, $\langle yE \rangle = -9.8$, $\langle yy' \rangle = 1.1$, $\langle yx \rangle = -0.7$, $\langle xE \rangle = -0.5$. Tuning knobs are not applied.

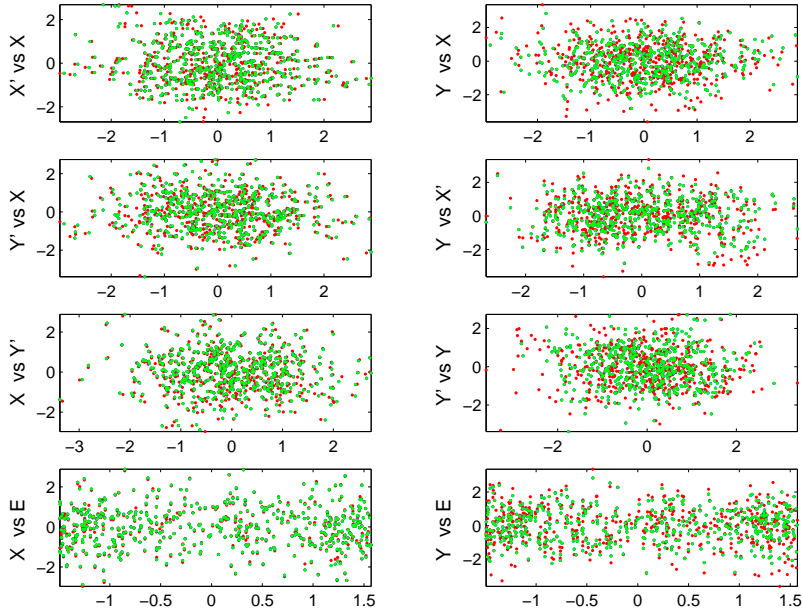


Figure 15: Beam phase-space at the IP determined by tracking. Green – ideal beam, red – the beam when the IP angle is compensated by the DID and offsets of QD0 and QF1 quadrupoles, and the beam size is corrected by linear knobs. The beam sizes are $\sigma_x/\sigma_{x0} = 1.00$, $\sigma_y/\sigma_{y0} = 1.028$, and all linear correlations are zeroed. Higher order tuning knobs are not applied.

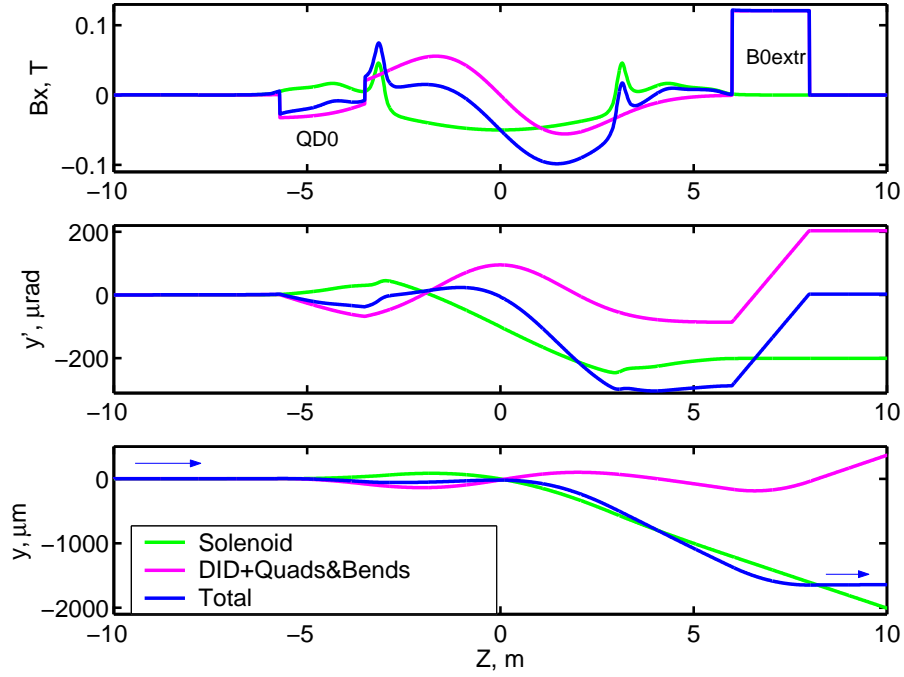


Figure 16: Beam orbits in SiD and post IP determined by integration of B_x , without tracking. The IP angle is compensated by DID Corrector and offsets of QD0 and QF1 and the extracted beam angle is compensated by a vertical bend.

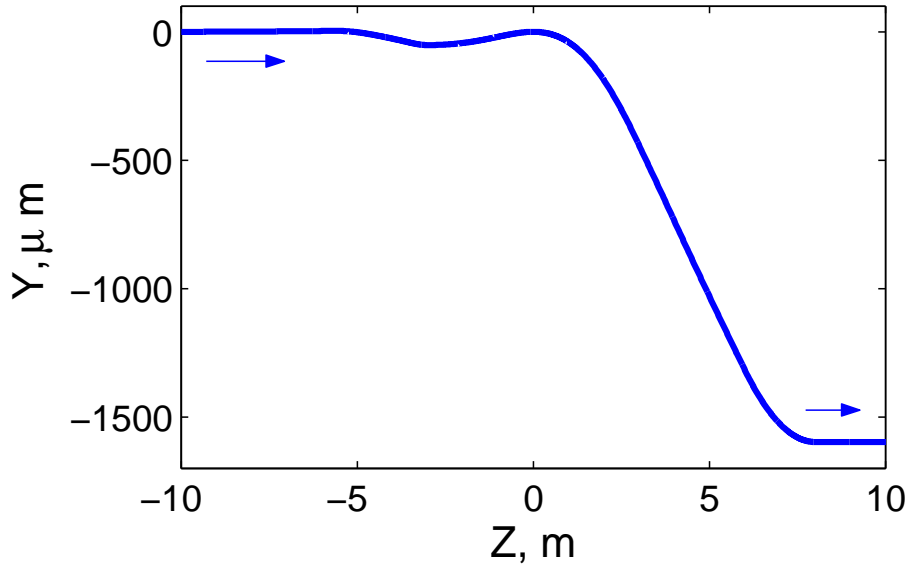


Figure 17: Beam orbits in SiD and post IP determined by tracking. The IP angle is compensated by the DID and FD offsets and the extraction beam angle is compensated by a vertical bend.

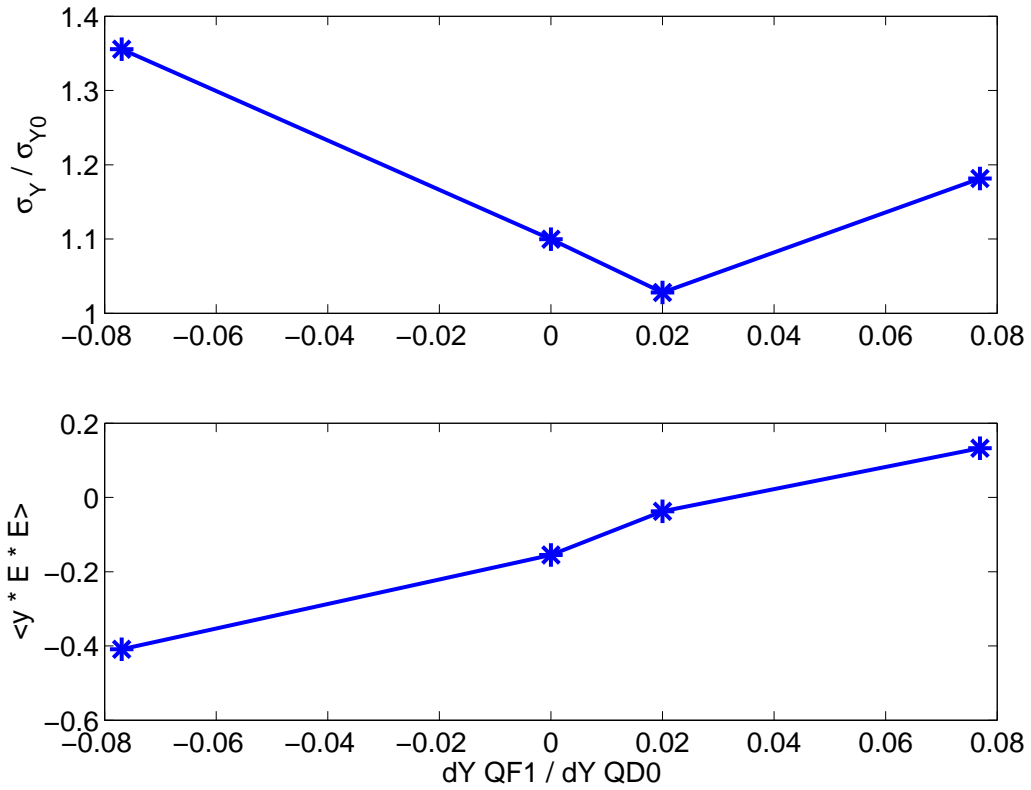


Figure 18: Beam size and second order vertical dispersion at the IP determined by tracking versus the ratio of offsets of QF1 and QD0 quadrupoles, which together with the DID Corrector compensate the IP beam angle.

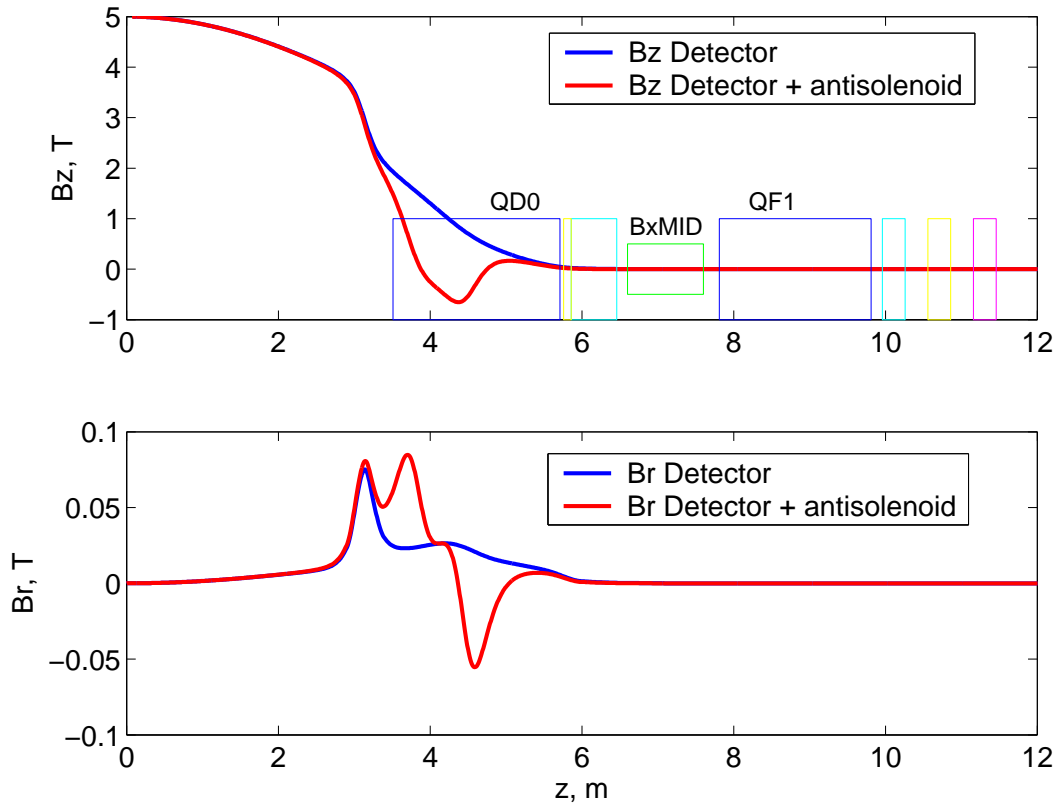


Figure 19: Fields of the Silicon Detector (SiD) calculated by ANSYS combined with the field of the antisolenoid which restore cancelation of the beam distortion by the solenoid field. Locations of the Final Doublet elements with additional middle dipole corrector BXMID are also shown.

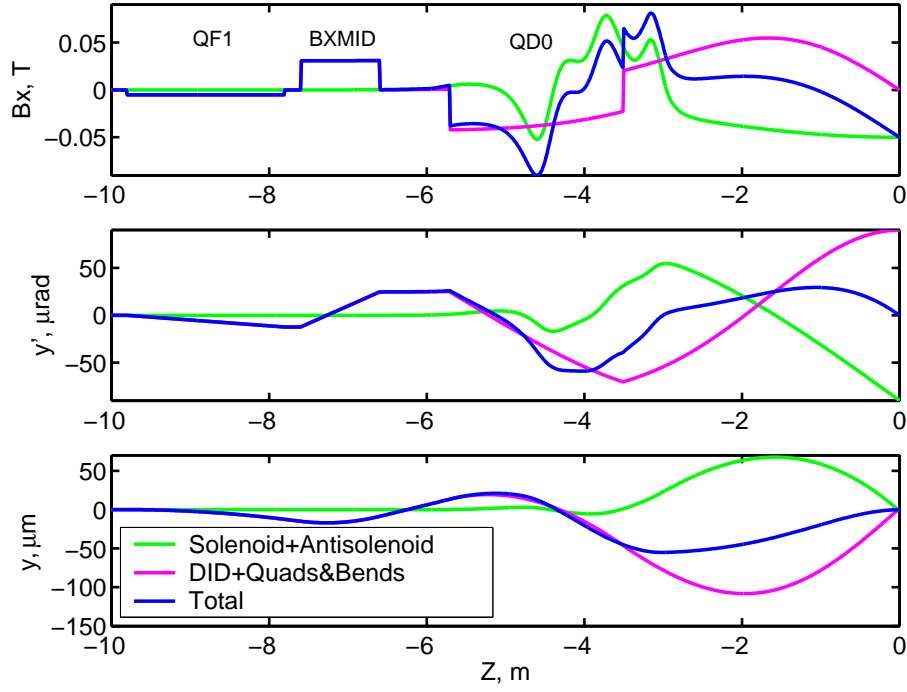


Figure 20: Beam orbits in SiD with antisolenoid determined by integration of B_x , without tracking. The IP angle is compensated by the DID, FD offsets and BXMID without introducing any linear or second order dispersion.

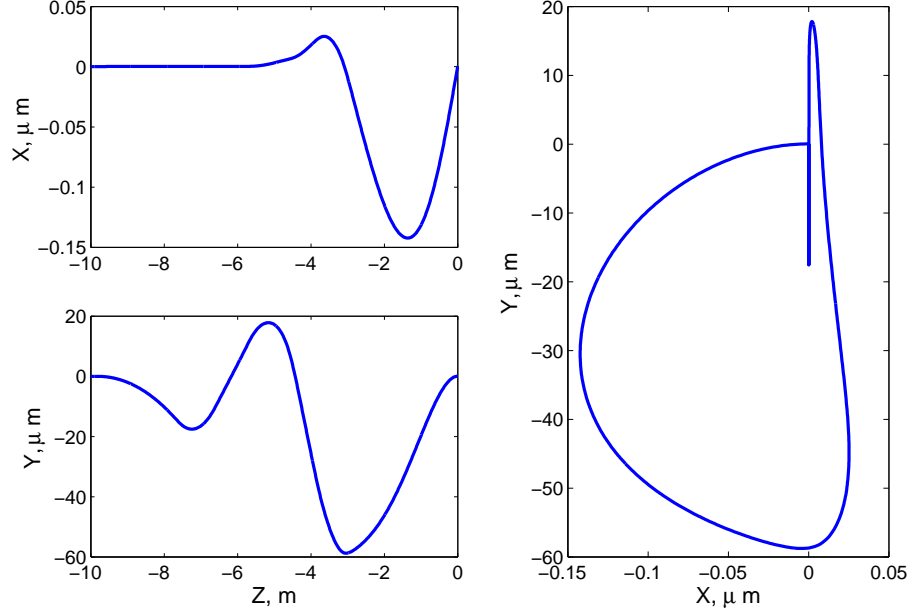


Figure 21: Beam orbits in SiD with antisolenoid determined by tracking. The IP angle is compensated by the DID, FD offsets and BXMID without introducing any linear or second order dispersion.

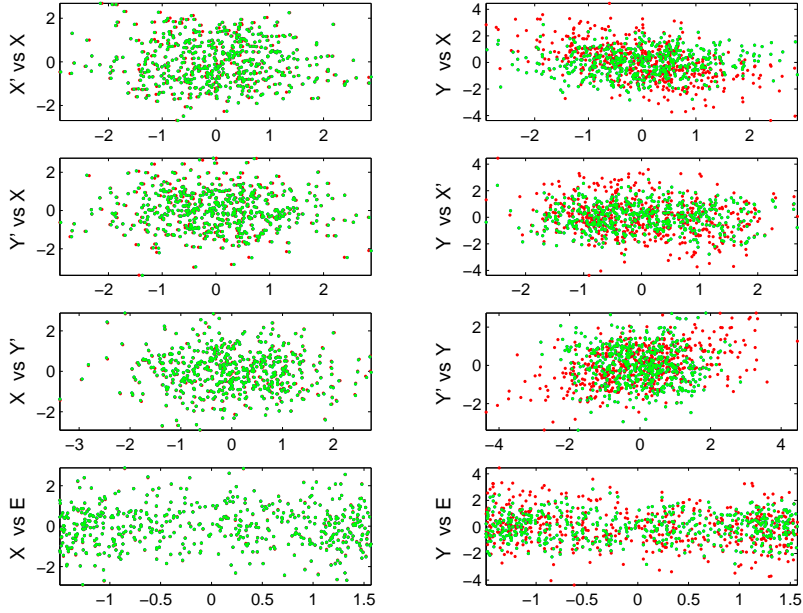


Figure 22: SiD with the antisolenoid and DID Corrector, no tuning knobs applied, beam phase-space at the IP determined by tracking. Green – ideal beam, red – the beam corresponding to the case when the IP angle is compensated by the DID, FD offsets and BXMID, and the knobs for beamsizes compensation are not applied. The beam sizes are $\sigma_x/\sigma_{x0} = 1.00$, $\sigma_y/\sigma_{y0} = 1.31$.

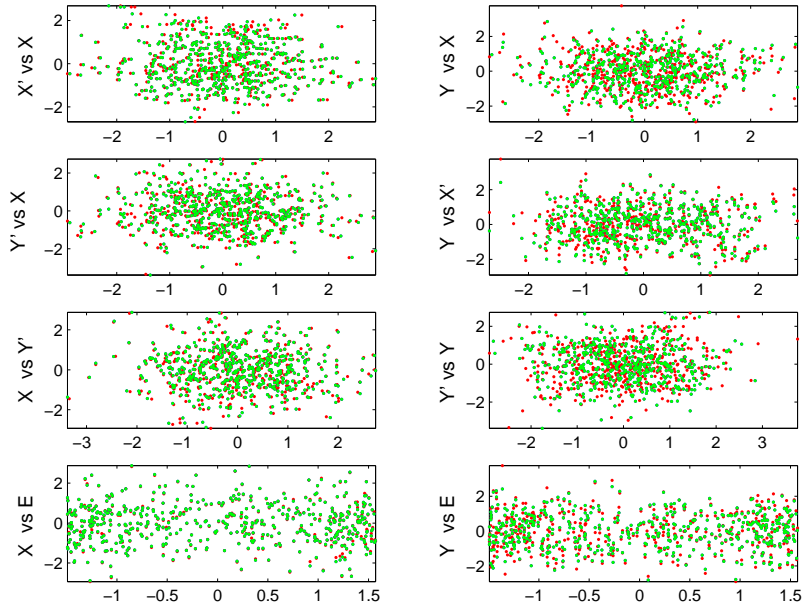


Figure 23: SiD with the antisolenoid and DID Corrector, linear tuning knobs are applied, beam phase-space at the IP determined by tracking. Green – ideal beam, red – the beam corresponding to the case when the IP angle is compensated by the DID, FD offsets and BXMID, and the beam size is corrected by linear knobs. The beam sizes are $\sigma_x/\sigma_{x0} = 1.00$, $\sigma_y/\sigma_{y0} = 1.01$, and all linear correlations are zeroed. No higher order tuning knobs were applied.

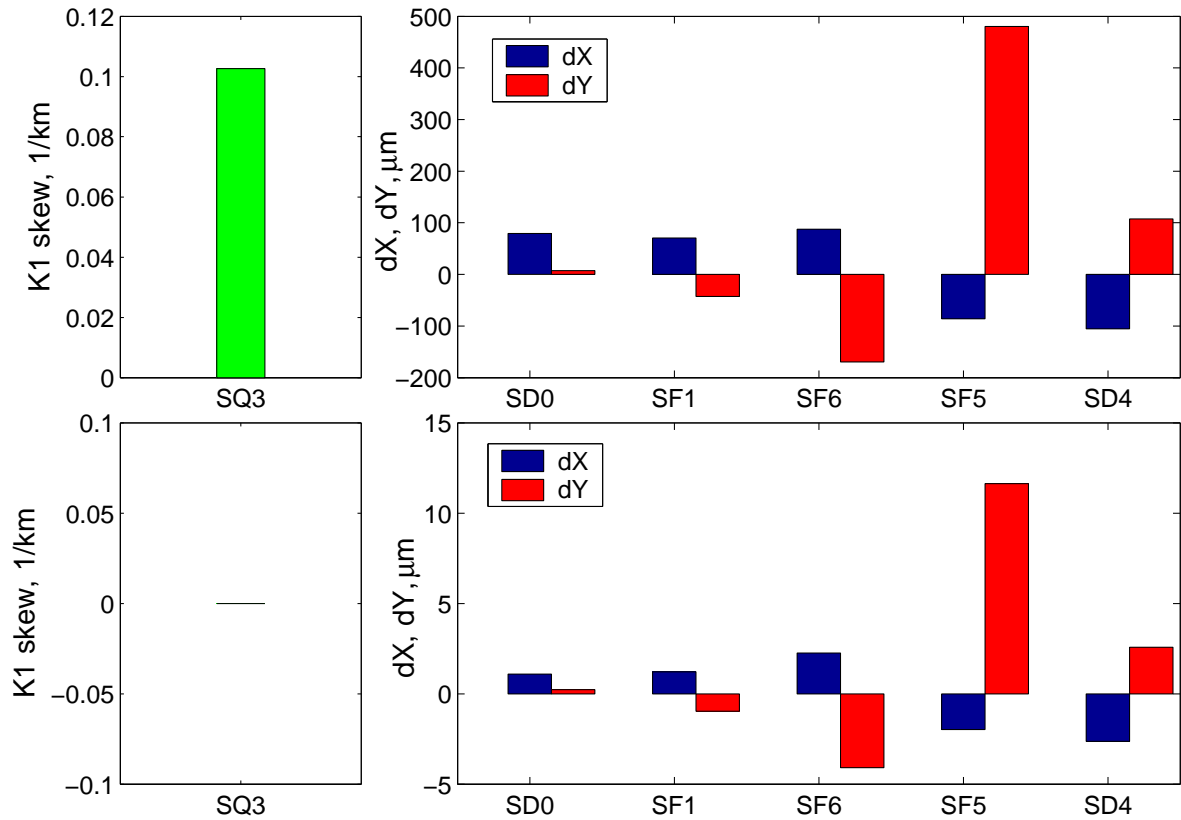


Figure 24: Strength of FD skew quadrupole SQ3 and displacements of sextupoles forming the linear knobs to correct the beam size at IP. Comparison of standard method of correction (two top plots) with the antisolonoid method (two bottom plots).

